Mechanisms of particle ejection from Cu(001) induced by the relative orientation of the bombarding primary ion

Karin E. Foley[a] and Barbara J. Garrison[a]

Department of Chemistry, The Pennsylvania State University, University Park, Pennsylvania 16802
(Received 16 July 1979; accepted 3 October 1979)

The effect of the angle of incidence of 600 eV Ar^+ ions on the yields and mechanisms of particle ejection from a clean Cu(001) and a $c(2\times2)$ overlayer of oxygen on Cu(001) has been examined. The total yield of particles ejected as a function of polar angle is in qualitative agreement with experiment. The azimuthal dependence of the yields for both the clean Cu(001) and Cu(001) with a $c(2\times2)$ overlayer has been predicted. Mechanisms of particle ejection which are specific to a particular angle of incidence have been identified. Of particular interest is a shearing mechanism which contributes to the ejection process at an angle of $\theta = 45°$ in the ⟨100⟩ directions. This shearing is responsible for the ejection of a large number of dimers which were originally next nearest neighbors on the surface. By energy selecting the dimers which eject, one can preferentially select the original sites of the two components. The angular distribution of the ejected particles, both substrate and adsorbate, due to normal incidence ion bombardment has previously been found to reflect the original surface site symmetry. The angular patterns of the ejected atoms are still dominated by the site sensitive effects, but the intensity is shifted due to the primary ion's off-normal angle of incidence.

I. INTRODUCTION

In recent years there has been extensive study of the interactions of ion beams (500–5000 eV) with solid surfaces. The incoming ion, depending upon its original direction, can either penetrate the solid or be blocked by surface atoms. This feature is exploited in channeling and backscattering experiments, where the crystallographic direction or the angle of incidence is chosen to either implant the ion into the crystal or to shadow atoms to gain structural information. Of particular interest here is the effect of the angle of incidence of the incoming primary ion on the ejection process.

Both experiments and theory have shown that the total yield of ejected particles varies considerably as a function of the incident angle of the incoming primary ion.[1] Harrison *et al.* have shown that changing the polar angle of incidence by as little as one-half of one degree can alter the yield as much as 20%.[2] In this study we wish to examine further the effect of the angle of incidence of the incoming ion, not only on total yields, but also on the mechanisms of ejection, cluster formation probabilities, and angular distributions.

Recent theoretical attempts to model the dissipation of the primary ion's momentum into the crystal have been very successful, both for giving a qualitative picture of the ion bombardment process and for calculating macroscopic experimental values.[3–7] This approach utilizes a standard classical dynamical treatment to model the response of a 240 atom microcrystallite to the impinging primary ion and is readily extendable to examine oblique angles of incidence of the primary ion.

One of the interesting conclusions drawn from this model for normal incidence ions is that there is considerable rearrangement of atoms in the observed clusters. That is, clusters are *not* formed from contiguous surface atoms which are ejected intact. However, Barber and Vickerman[8] have shown for a 2-dimensional solid that considerable shearing or peeling off of layers occurs for oblique angles of incidence, and thus there should be a high probability of neighboring atoms forming clusters. We would like to discern, then, whether the shearing is a mechanism of ejection at oblique angles or whether Barber and Vickerman's shearing was due to artificially constraining the momentum to one plane. An obvious ramification of this phenomenon is that by analyzing the dimers ejected from an alloy surface one could conceivably determine which types of atoms were neighbors and thus something of the amount of local arrangement of atoms on the surface.

Thus, in this paper we will discuss the effect of varying the angle of incidence of the primary ion beam, both polar and azimuthal angles, on the mechanisms and yields of particles ejected from a clean copper(001) face. In addition, we will analyze the effect of varying the azimuthal angle at a polar angle of 45° on the ejection process of a $c(2\times2)$ coverage of atomic oxygen on a copper(001) face.

II. DESCRIPTION OF THE CALCULATION

The dynamics of the ion bombardment process have been modeled classically, thus allowing the position and momentum of each particle to be followed as a function of time. From the details of each particle's motion we can determine quantitative information such as yields, cluster formation probabilities, energy distributions, and angular distributions.

The infinite solid is approximated by a microcrystallite of ~240 atoms, four layers of ~60 atoms/layer.[3] Additional atoms can be placed on the surface to model adsorbates.[5,6] For the calculations presented here, the solid is a copper crystal with the (001) face exposed to the ion beam. In some cases a $c(2\times2)$ or half monolayer coverage of atoms with the mass of oxygen has been included. These atoms are placed in a fourfold bridge configuration at an equilibrium height of 1.74 Å above

[a]Work performed at: Department of Chemistry, Purdue University, West Lafayette, IN 47907.

 0021-9606/80/021018-10$01.00

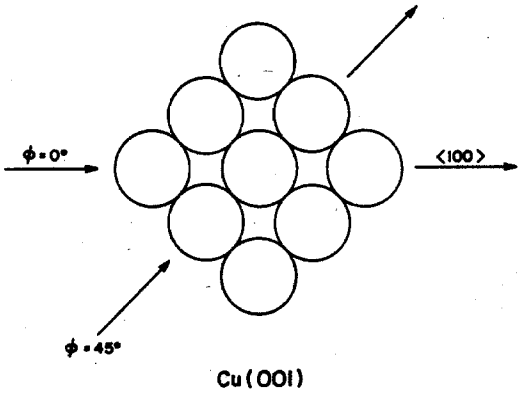

FIG. 1. Cu(001) showing the azimuthal directions. The actual microcrystallite used in the calculations contained 61 atoms/layer rather than 9.

the surface plane and are bound by 0.75 eV to the surface.

The primary ion in all cases is Ar^+ with an initial energy of 600 eV. Its polar angle with respect to the normal, θ, and azimuthal angle, ϕ, are then varied. The value of $\phi = 0°$ corresponds to the ⟨100⟩ directions and $\phi = 45°$ to the ⟨110⟩ directions as shown schematically in Fig. 1. The Ar^+ is allowed to impact the surface at various points in an impact zone appropriate to the symmetry of the crystal face and overlayer and the angle of incidence of the ion. A total of 100 different impact points or Ar^+ trajectories are calculated for each angle of incidence to provide the necessary averages for computation of statistically reliable yields. The solid is assumed to be at 0 K.

With the above initial conditions, Hamilton's equations of motion are integrated in time to yield the final positions and momenta of all the particles. For the interaction potential among the particles, a pairwise additive function was used. The metal–metal, metal–adsorbate, and adsorbate–adsorbate potentials are represented by a repulsive Born–Mayer function at small internuclear separations splined to an attractive Morse potential at long range. A purely repulsive potential is used to represent the interaction of Ar^+ with the other species. The exact functional forms and parameters of all the potentials have been given previously.[5,6]

The collision cascade is terminated when the most energetic copper or oxygen atom left in the crystal has less than 2 or 1 eV, respectively, of energy and no more particles can eject. The ejected particles are then analyzed for yields, possible cluster formation,[4,5] energy distributions, and angular distributions.

It is of interest to compare some of the details of the approach used here to thermal gas phase collisions. Typically in dynamics calculations of gas phase collisions, thousands of trajectories need to be calculated since many initial conditions must be averaged and relatively few trajectories produce the desired experimental observable. For this ion–solid system only the two coordinates of the impact point on the surface need to be averaged. The final conditions are relatively slowly varying functions of the impact coordinates and for many experimental observables, nearly all the trajectories are successful. As a consequence fewer sets of initial conditions (50–200) need to be used. This does not decrease the total computer time, however. Each impact point takes ~30–45 s on a CDC 7600.

We generally choose the impact points in an ordered grid over the impact zone which represents the crystal face and overlayer symmetry. Points on the edges of the impact zone tend to produce nonrepresentative sampling so whenever possible we pick points in the interior of the impact zone. An example of this is normal incidence Ar^+ on the (001) face of a face centered cubic crystal where edge points along the ⟨100⟩ azimuth produce a low yield. For 1 keV Ar^+ on Ni(001) one sample of ~100 impact points, including edge points, gives a yield of 4.4. Another set of ~100 interior points gives a yield of 4.8, while a sample of 1255 impact points predicts the yield to be 4.65 ± 0.06.[9] These differences are systematic. Trends of observables as a function of primary ion energy, angle, and crystal mass can be predicted with higher reliability than absolute quantities, if the same set of impact points are used. In this study we have used a consistent set of points in the interior of the impact zone. Counting statistics have been used to determine error bars at the 68% confidence level. We feel that the trends are more accurately determined, however, due to the consistent set of impact points.

In thermal gas phase classical trajectories a high order (4th or greater) predictor–corrector is used so that large time steps may be taken. For the keV processes, the forces are changing so rapidly that they limit the time step size and a low order predictor–corrector is considerably faster. An integrator, which has been described previously,[10] is used with a modification to pick the new time step based on the difference in the predictor and corrector values of the previous step.[11] At the beginning of the trajectory the time step is typically $\sim 10^{-16}$ and eventually increases to $\sim 10^{-14}$ s. A total of 100–200 integration steps are taken.

The consistency of the physical observables with changes in integrator tolerance or step size is the criterion for determining the accuracy of the integrator. Changing the final step size by a factor of 5 only alters the final positions and momenta of the particles by 1%–2%. Naturally this increases the total computer time considerably. We feel this error is quite tolerable given the approximate interaction potential used in this procedure.

The termination of the trajectory is based on the energy of the particles remaining in the solid. By making the cutoff energy smaller, the trajectory runs longer. The cutoff energies (2 eV for Cu and 1 eV for O) are chosen so that all particles have ejected. Properties such as yield, energy distribution, and angular distribution are affected little by this choice. The most sensitive observable is the cluster formation probabilities. Since the pair potentials used for the bulk dynamics do not dissociate correctly, we use gas phase

TABLE I. Clean Cu(001). Dependence of the number of species ejected on the polar angle θ for a fixed azimuthal angle $\phi = 0°$.

θ =	0°	15°	30°	45°	60°
Number of impact points	111	100	100	100	100
Ar^+	102	80	81	100	100
Ar^+ yield	0.9	0.8	0.8	1.0	1.0
Cu	436	446	474	414	190
Cu yield	3.9	4.5	4.7	4.1	1.9
Cu_2	17	27	20	29	12
Cu_3	3	2	1	4	0

[a]The yields are correct to approximately ± 0.2.

TABLE III. Energy distributions for clean Cu(001). Percent of monomers that eject within a given energy range as a function of polar angle θ for a fixed azimuthal angle $\phi = 0°$.

θ =	0°	15°	30°	45°	60°
Cu					
< 10 eV	56	61	56	65	88
10–20 eV	17	20	18	19	10
> 20 eV	27	29	26	16	21
Ar^+					
< 10 eV	53	53	51	25	0
10–20 eV	28	20	11	13	0
> 20 eV	19	27	38	62	100

potentials to analyze for clusters.[4,5,13] Although the exact cutoff energy is not extremely critical, the same energy must be used for all calculations in order to have a consistent comparison.

III. RESULTS AND DISCUSSION–CLEAN Cu(001)

A. Yields

Variations in the ejection yields (number of particles ejected per incident ion) as a function of polar angle θ and azimuthal angle ϕ are given in Tables I and II. For the polar angle variation, ϕ was held fixed at 0°, while for the azimuthal angle variation, θ was held at 45°. Figure 2 graphically displays the variations in yield with angle.

The variations in yield with polar angle can easily be explained by considering the bombardment mechanism. As the polar angle increases, the incident Ar^+ ion has a decreasing amount of vertical momentum. The vertical momentum, in general, is more easily transferred to the crystal while the horizontal momentum is more easily retained by the primary ion. This is supported by the fact that at $\theta = 0°$, 81% of the ejected Ar^+ ions have less than 20 eV of energy, while at $\theta = 60°$, 0% of the Ar^+ ions are ejected with an energy of less than 20 eV (see Table III). Conversely, at $\theta = 0°$, 73% of the ejected Cu atoms have less than 20 eV of energy, while at $\theta = 60°$, 98% of the ejected Cu atoms have less than 20 eV. Also shown in Fig. 2(a) are experimental yields from 20 keV Ar^+ bombardment of Cu(001).[12] The calculations and experiments exhibit qualitatively the same behavior. The experimental values, however, show considerably larger variations, possibly due to the larger incident energy of the Ar^+. Harrison *et al.* have indicated that higher angular resolution is needed to obtain the small fluctuations in the total yield.[2]

TABLE II. Clean Cu(001). Dependence of the number of species ejected on the azimuthal angle ϕ for a fixed polar angle $\theta = 45°$.

ϕ =	0°	11.25°	22.50°	33.75°	45°
Number of impact points	100	100	100	100	100
Ar^+	100	96	98	94	95
Ar^+ yield	1.0	1.0	1.0	0.9	1.0
Cu	414	419	476	476	503
Cu yield	4.1	4.2	4.8	4.8	5.0
Cu_2	29	28	23	18	28
Cu_3	4	1	4	3	3
Cu_4	0	0	1	1	3

[a]The yields are correct to approximately ± 0.2.

The variation in total yield with azimuthal angle shows a slight increase as ϕ increases from 0° to 45°. The lower yield occurs when the Ar^+ ion bombards in the loosely packed ⟨100⟩ directions. When the Ar^+ ion bombards along the close packed ⟨110⟩ directions, the efficiency of momentum transfer is increased and more atoms are ejected. A similar effect has been noted earlier, where ~50% more particles ejected from the closely packed (111) face than the (001) face.[3] To our knowledge the variation of yield with azimuthal angle has not been measured, but experimental verification should be relatively straightforward.

The distribution of ejected atoms as a function of their

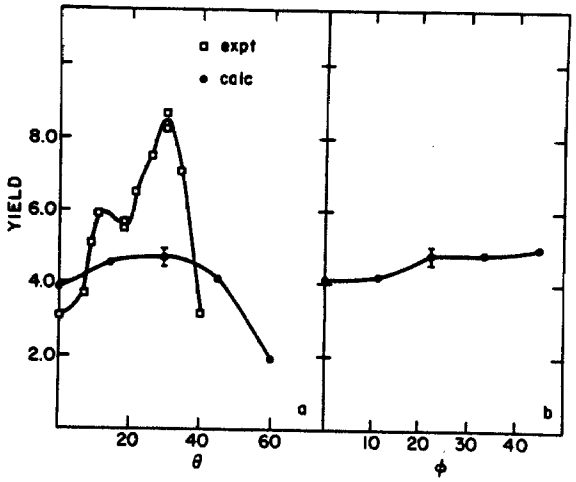

FIG. 2. Yield of ejected copper atoms. (a) Versus polar angle θ for $\phi = 0°$. Both the calculated yield and the experimental yield of Ref. 12 are shown. (b) Versus azimuthal angle ϕ for $\theta = 45°$. Only the calculated yield is shown.

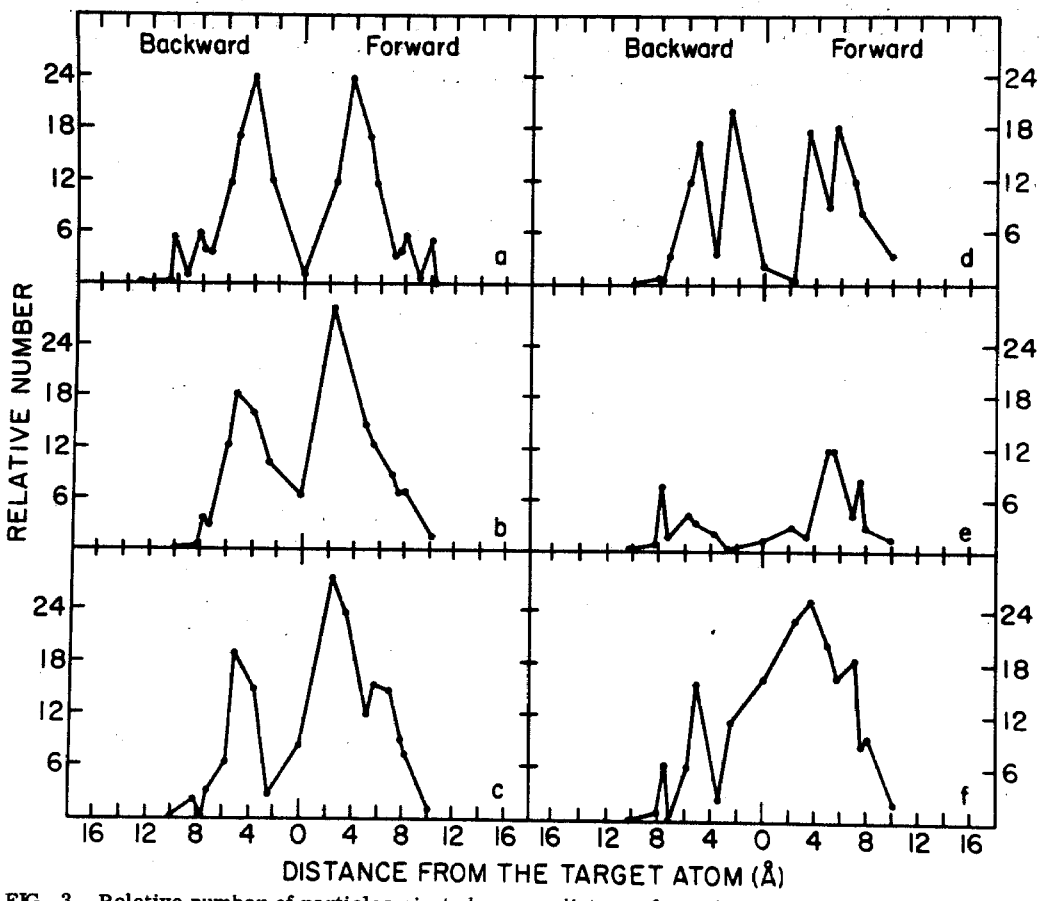

FIG. 3. Relative number of particles ejected versus distance from the target atom. The points represent the percent of ejected particles per distance unit. The lines are only meant as a guide to the eye and have no physical significance. The descriptions "forward" and "backward" denote regions on either side of an imaginary plane perpendicular to the plane of the incident Ar^+ ion and passing through the target surface atom. The positions of the points are the distances of the atoms in the surface from the target atom, thus there is an uneven spacing. (a) $\theta = 0°$, $\phi = 0°$; (b) $\theta = 15°$, $\phi = 0°$; (c) $\theta = 30°$, $\phi = 0°$; (d) $\theta = 45°$, $\phi = 0°$; (e) $\theta = 60°$, $\phi = 0°$; (f) $\theta = 45°$, $\phi = 45°$.

original distance from the target atom yields some insight as to which ejection mechanisms predominate at various polar and azimuthal angles. Figure 3 shows the systematic change in the damage cross section as the polar angle varies from 0° to 60°. The descriptions "forward" and "backward" denote regions on either side of an imaginary plane perpendicular to the plane of the incident Ar^+ ion and passing through the target surface atom. As θ varies from 0° to 30°, the number of atoms ejected from the forward region increases over the number ejected from the backward region. This is a result of an increasing horizontal component of momentum being transferred into the crystal. Most of the momentum is in the forward direction, and as a result more particles eject from the forward region. These particles generally have higher kinetic energies. As discussed above, as θ increases from 30° to 60° the yields from both the forward and backward regions become significantly lower. At $\theta = 45°$, the forward damage cross section has two distinct peaks with the maximum intensity shifting to distances further from the target atom in the forward direction. These changes can be attributed to a shearing effect. The target atom is struck at such an angle that it can move between the first and second layers, ejecting the surface atoms above it. In addition, other atoms exhibit a similar shearing mechanism. This shearing thus accounts for the changes in the features of the damage cross sections. It will be discussed further in the section on cluster formation.

The difference in the damage cross sections of $\theta = 45°$, $\phi = 0$ and $\theta = 45°$, $\phi = 45°$, is shown in Fig. 3(d), (f). The shape of the plot for $\theta = 45°$, $\phi = 0$ has been discussed above. A large increase in the forward intensity is observed when $\theta = 45°$, $\phi = 45°$. These angles correspond to the Ar^+ ion bombarding the crystal along the close packed rows in the (001) face ($\langle 110 \rangle$ directions). This provides a very efficient mechanism for momentum transfer[3] and accounts for the large increase in ejection yield from the forward direction.

Thus, it has been shown that the polar and azimuthal angles at which the surface is bombarded alter the distribution and mechanisms of particle ejection. The effect of the oblique angles of incidence on the mechanisms and yields of cluster formation will now be discussed.

B. Cluster formation

Clusters from ion bombarded surfaces have been previously shown to form by a recombination of ejected atoms in the near surface region rather than by ejec-

tion of intact entities from the surface.[13] We find that for oblique angles this conclusion continues to be valid. However, we do find new mechanisms of cluster formation that arise because the Ar^+ ion is bombarding at oblique angles.

Shown in Fig. 4(a) is the copper dimer to monomer ratio as a function of polar angle θ. Note that the ratios differ by as much as a factor of two. We believe these differences to be statistically significant and ascribe them to mechanisms that cause dimer formation unique to a specific angle of incidence of the primary ion. For example, at $\theta = 45°$ we find that 10 out of 29 dimers form via a shearing mechanism similar to that shown in Fig. 5(a). For this particular trajectory the Ar^+ ion strikes atom No. 1 which moves between the first and second layers at an angle of ~15° with respect to the surface. As No. 1 moves along it pushes up on atoms Nos. 2–5 while pushing down on atoms Nos. 6–9. Two dimers are subsequently formed, one composed of atoms No. 3 and No. 5 which has kinetic energy of 7 eV and one composed of atoms No. 2 and No. 4 which has kinetic energy of 20 eV.

The shearing mechanism is characteristic of $\theta = 45°$. However, for other polar angles other distinctive mechanisms can contribute to dimer formation. For example, at an initial polar angle of 15° a different characteristic ejection mechanism is responsible for the formation of 6 out of 27 dimers. This mechanism is shown schematically in Fig. 5(b). The Ar^+ ion impinges between atoms No. 1 and No. 2. Atom No. 2 moves down, pushing up No. 3. The Ar^+ meanwhile reflects off atom No. 5 in the second layer and ejects No. 4. Atoms No. 3 and No. 4 subsequently form a dimer. Another characteristic mechanism occurs when $\theta = 60°$ where 5 out of 12 dimers arise from the Ar^+ ion striking contiguous impact points. This particular mechanism is shown schematically in Fig. 5(c). The Ar^+ ion strikes atom No. 1 causing it to move at an angle of ~45° with respect to the surface towards atom No. 4. Atom No. 4 moves down, pushing No. 6 up which then ejects No. 2 from behind. In the meantime, atom No. 1 starts moving under atom No. 5 pushing it up and thus ejecting atom No. 3. The dimer is formed from atoms No. 2 and No. 3.

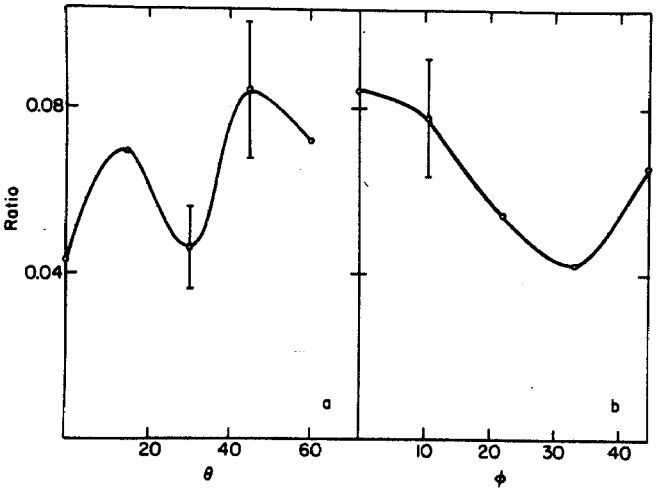

FIG. 4. Copper dimer to monomer ratio. (a) Versus the polar angle θ for $\phi = 0°$. (b) Versus the azimuthal angle ϕ for $\theta = 45°$.

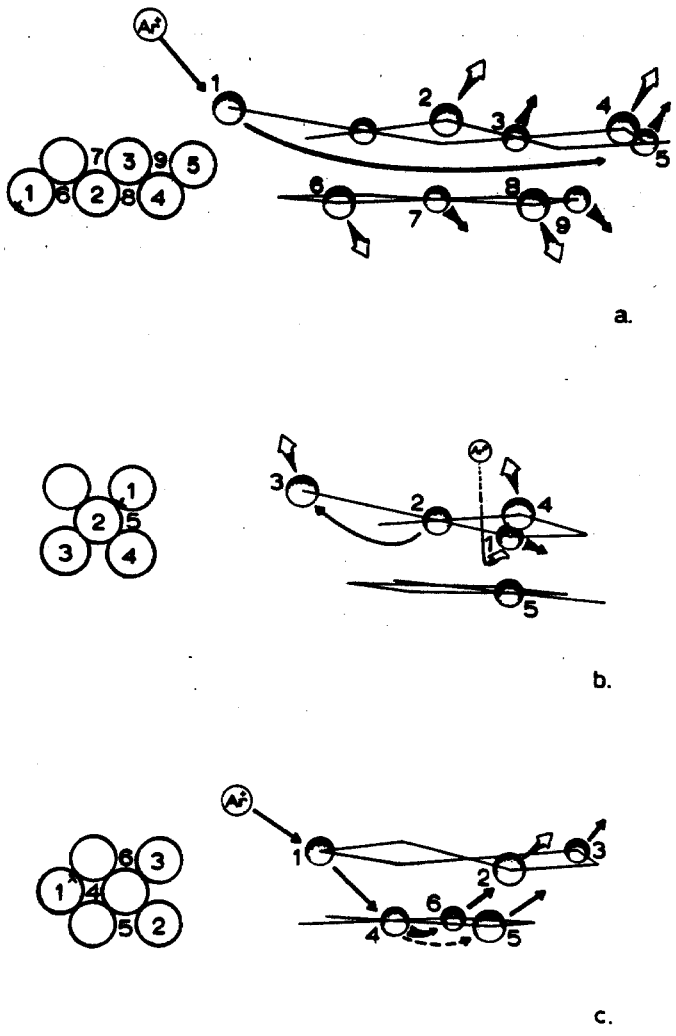

FIG. 5. Mechanisms of dimer formation. Only the atoms involved in the ejection of the indicated atoms are drawn. The actual size of the crystallite used in the calculation is considerably larger but is not shown for graphical clarity. The arrows indicate the approximate direction of motion of each atom during the trajectory. The numbers near the atoms are simply used as labels (see text). The left side of each frame shows the position of each atom in the original surface layer with the x being the impact point of the Ar^+ ion. Other atoms are located at the intersection of the grid lines, which are the nearest neighbor bonds of the (001) crystal face.

If one were to arbitrarily remove the above described dimers from the total dimer yield and attribute the remainder of the dimer formations to "random" processes, one would find that the copper dimer to monomer yield as a function of angle θ is nearly constant. It is quite feasible, in addition, that more detailed structure would be present if a higher angular resolution were obtained.

One interesting observation is that all three of the above described mechanisms give rise to dimers that form from atoms which were originally next nearest neighbors on the surface. A detailed analysis of the

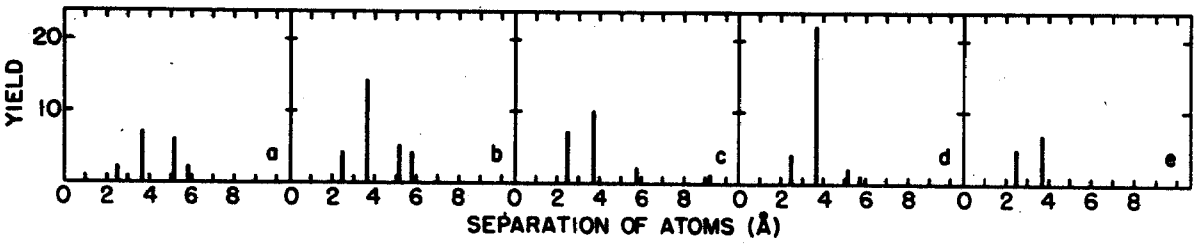

FIG. 6. Yield of dimers versus original separation of constituent atoms on the surface. The nearest neighbor separation on copper is 2.56 Å. The positions of the lines are the separation distances of the atoms in the surface. (a) $\theta = 0°$, $\phi = 0°$; (b) $\theta = 15°$, $\phi = 0°$; (c) $\theta = 30°$, $\phi = 0°$; (d) $\theta = 45°$, $\phi = 0°$; (e) $\theta = 60°$, $\phi = 0°$.

original distance between constituent atoms of the dimers is given in Fig. 6. As the polar angle increases the percent of dimers that were originally next nearest neighbors (3.62 Å) greatly increases, particularly at $\theta = 45$, where the shearing mechanism plays a dominant role.

The variation in the dimer to monomer ratio as a function of azimuthal angle is shown in Fig. 4(b). These ratios also differ by more than a factor of 2. The peak at $\theta = 45°$, $\phi = 0°$ has been described above. At $\theta = 45°$, $\phi = 45°$ there seems to be an increase in nearest neighbor dimers (see also Fig. 7). Careful perusing of the trajectories does not yield a single preferred mechanism. Rather, ion bombardment parallel to the close packed rows tends to increase the number of dimers, particularly those which are nearest neighbors. There does not appear to be any shearing at $\phi = 45°$.

The observation that there is a high probability of forming dimers from next nearest neighbors when the angle of incidence is in the $\phi = 0°$ or $\langle 100 \rangle$ directions and from nearest neighbors when the angle of incidence is in the $\phi = 45°$ or $\langle 110 \rangle$ directions is similar to the results for the normal incidence studies on different crystal faces.[4] The results for normal incidence on Cu(001) are shown in Fig. 6(a). Here there are few nearest neighbor dimers. For Ar^+ normally incident on Cu(111) the dimer distribution is more nearly represented by Fig. 7(e).[4]

Although the number of trimers formed in each case is small and their statistics somewhat unreliable, the mechanism of their formation does warrant some discussion. Studies of Cu(001) crystals bombarded at normal incidence have shown that trimers almost always contain at least one nearest-neighbor pair, and thus reflect a large amount of local order.[4] This has not been found to be true in these oblique angle studies. Although these trimers still originate from within an area of radius ~5 Å, they are not composed of as many nearest neighbor atoms as were the trimers found in the normal incidence studies.

Our basic conclusions regarding cluster formation are not altered by these oblique angle studies. The clusters still form in the near surface region and show considerable rearrangement from their initial positions on the surface. They also originate from a localized area of radius ~5 Å. However, new mechanisms begin to dominate as the ion bombards at different angles. Of particular interest is the apparent shearing that occurs when the Ar^+ ion strikes at $\theta = 45°$ and $\phi = 0°$, causing a relatively large number of dimers which were originally next nearest neighbors on the surface to be formed.

C. Energy distribution

The shape of the energy distribution curves for the ejected copper monomers due to Ar^+ ion bombardment at oblique angles is very similar to that for the normal incident Ar^+ ion.[3,14] Basically the distribution starts at zero, peaks at an energy of ~2 eV, and then tails off with a maximum energy of ~200 eV for normal incidence Ar^+. There are a few differences, however, particularly in the higher energy part of the distribution.

Rather than graphing the energy distributions, which have considerable statistical noise, the salient features are given in Table III. This table gives the percent of monomers which are ejected with less than 10 eV, between 10 and 20 eV, and with more than 20 eV of energy, for both Cu and Ar^+. As θ increases the percent of ejected Cu monomers with less than 10 eV of energy increases from ~60% to ~90% while the high energy fraction (>20 eV) decreases from 27% to 2%. Less energy

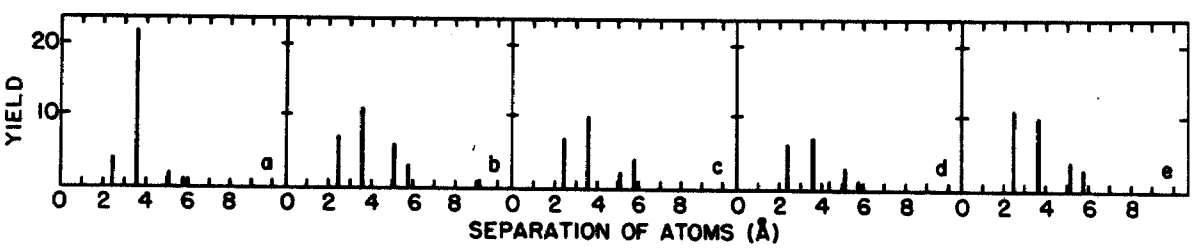

FIG. 7. Yield of dimers versus original separation of constituent atoms on the surface. (See explanation of Fig. 6.) (a) $\theta = 45°$, $\phi = 0°$; (b) $\theta = 45°$, $\phi = 11.25°$; (c) $\theta = 45°$, $\phi = 22.50°$; (d) $\theta = 45°$, $\phi = 33.75°$, (e) $\theta = 45°$, $\phi = 45°$.

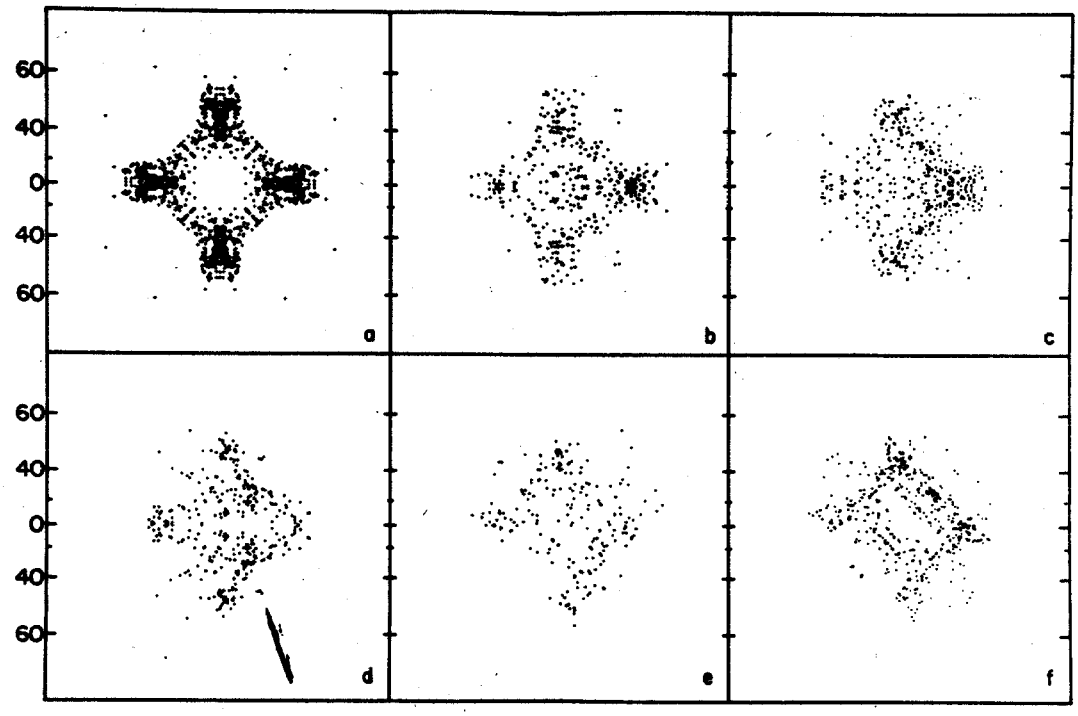

FIG. 8. Angular distributions of the ejected copper atoms. Each ejected atom is plotted on a flat-plate collector an arbitrary distance above the crystal. In all cases only those atoms with greater than 10 eV of kinetic energy are shown. The numbers on the ordinate refer to the polar deflection angle given in degrees. The orientation of the crystal is the same as in Fig. 1. (a) $\theta = 0°$, $\phi = 0°$; (b) $\theta = 15°$, $\phi = 0°$; (c) $\theta = 30°$, $\phi = 0°$; (d) $\theta = 45°$, $\phi = 0°$; (e) $\theta = 45°$, $\phi = 22.5°$; (f) $\theta = 45°$, $\phi = 45°$.

is going into the crystal at $\theta = 60°$ and thus not as many high energy Cu atoms are ejected. The ejected Ar^+ ions show exactly the opposite trend. The number of low energy Ar^+ ions (< 10 eV) decreases from 53% to 0% as θ goes from 0° to 60°. At $\theta = 60°$, however, all the ejected Ar^+ have greater than 20 eV of energy. There is virtually no difference in either the Cu or Ar^+ energy distributions as a function of azimuthal angle.

Of special interest is the energy distribution of the ejected dimers. In the trajectory of Fig. 5(a), the two dimers that were ejected due to the shearing mechanism had relatively high kinetic energy. For the initial Ar^+ angles of $\theta = 45°$ and $\phi = 0°$ the average center of mass kinetic energy of all next nearest neighbor dimers is 8.5 eV, while the remainder of the dimers have an average energy of 5.5 eV. By only analyzing for dimers with greater than 5 eV of energy we find that the ratio of the number of next nearest neighbor dimers to the number of other dimers is ~2.3 whereas if one analyzes dimers of all energies this ratio is ~1.7. Thus by energy selecting the dimers, one can preferentially select the original sites of the two components.

A similar analysis can be done for the nearest neighbor dimers ejected with an initial Ar^+ direction of $\theta = 45°$ and $\phi = 45°$. By energy selecting the dimers in the range of 6–12 eV we find the ratio of nearest neighbor dimers to the rest is ~2.3 while without energy selection this ratio is ~0.6. There is an upper limit of 12 eV due to a few very high energy (15–40 eV) dimers which do not originate as nearest neighbors.

The experimental ramifications of these predictions are clear. By carefully selecting the angle of incidence of the primary ion beam and the energy of the ejected dimers, one can preferentially enhance the relative number of nearest or next nearest neighbor dimer pairs. This could be particularly important in studying the surface structure of alloys.

D. Angular distributions

The angular distributions of the high energy ejected particles have been shown to strongly reflect the original surface position of the atoms.[15,16] These high energy particles generally eject early in the collision cascade, when there is a considerable amount of surface structure still present. Thus they reflect the symmetry of the crystal face and the arrangement of the atoms on the surface.

We have chosen to display the angular distributions of the ejected atoms on a flat-plate collector an arbitrary distance above the crystal as shown in Fig. 8. In all cases only those atoms with greater than 10 eV of kinetic energy are shown. The radial distance corresponds to the polar deflection angle. The orientation of the crystal is the same as in Fig. 1.

Figure 8(a) displays the copper angular distribution for normal Ar^+ ion incidence. There are four regions of high intensity of ejected atoms. These arise due to the Cu ejecting in the direction of the fourfold holes surrounding it (Fig. 1). As the polar angle is increased from $\theta = 15°$ to $\theta = 45°$ [Figs. 8(b)–(d)], the pattern becomes more intense in the forward direction and less intense in the backward direction. For $\theta = 60°$, the pat-

TABLE IV. Oxygen on Cu(001). Dependence of the number of species ejected on the azimuthal angle ϕ for a fixed polar angle $\theta = 45°$.

ϕ =	0°	11.25°	22.50°	33.75°	45°	Normal incidence
Number of impact points	100	100	100	100	100	121
Ar^+	97	97	96	96	99	106
Ar^+ yield	1.0	1.0	1.0	1.0	1.0	0.9
Cu	342	345	398	327	351	416
Cu yield	3.4	3.5	4.0	3.3	3.5	3.4
O	663	689	711	734	635	607
O yield	6.6	6.9	7.1	7.3	6.4	5.0
Cu_2	12	13	21	12	13	13
O_2	17	13	16	11	6	19
CuO	29	23	35	28	20	34

[a]Also observed are the larger clusters Cu_3, Cu_2O, CuO_2, O_3, Cu_4, Cu_3O, Cu_2O_2, CuO_3, Cu_2O_3, Cu_3O_2, Cu_4O, Cu_3O_3, Cu_5O_3. The yields are correct to approximately ±0.2.

tern is the same, but the total yield is much lower. The basic angular distribution or the azimuthal position of the regions of high intensity are not altered by an oblique angle of incidence. The surface structure continues to play a dominant role in directing the ejecting particles.

The angular distributions of the copper atoms as a function of azimuthal angle are shown in Figs. 8(d)–(f). Even for $\phi = 45°$, which would tend to force the atoms to eject in the same $\phi = 45°$ direction, the regions of high intensity in the ⟨100⟩ directions remain.

IV. RESULTS AND DISCUSSION–OXYGEN ADSORBED ON Cu(001)

A. Yields

The ejection yields for oxygen adsorbed on Cu(001) as a function of azimuthal angle ϕ, for θ fixed at 45°, are given in Table IV. Both Cu and O yields are reasonably constant as a function of ϕ. As in the case of the normal incidence studies,[5] the copper yield is reduced by ~20% by adsorbing the half monolayer of oxygen. The oxygen yield for oblique angles of incidence is enhanced by 20%–40% over the normal incidence yield. These yields have not to our knowledge as yet been measured.

The distribution of ejected atoms as a function of the original distance from the target atom is shown in Fig. 9 for both the copper and the oxygen. The copper curves are fairly similar to the clean metal results (cf. Fig. 3). However, a larger percentage of the copper atoms eject from the forward direction when the oxygen adsorbates are present. The oxygen curves show that an oxygen has the highest probability of ejecting when it is closest to where the Ar^+ strikes. A considerable number of oxygen atoms eject from near the edge of the microcrystallite, a distance of 10–12 Å from the target atom. Testing of a few trajectories with larger crystallites indicates that most of the edge oxygens are ejecting with low kinetic energy and are unable to subsequently eject other atoms at a further distance from the target atom. Thus the distributions shown in Fig. 9(c), (d) will drop quickly to zero and 85%–90% of the ejected oxygen atoms have been accounted for.

B. Cluster formation

As in the studies for normally incident Ar^+ ion bombardment of oxygen on Cu(001), an abundance of clusters are formed. These range from the dimers, Cu_2, O_2, and CuO, and trimers, Cu_3, Cu_2O, CuO_2, O_3, to clusters as large as Cu_5O_3. The mechanism for the formation of these clusters is the same as discussed above; that is, the atoms eject and recombine in the near surface region.

The dimer yields do show some dependence on the original angle of incidence. The Cu_2/Cu, O_2/O, CuO/O, and CuO/Cu ratios are displayed in Fig. 10. The variation can be as large as 50%. Extensive perusing of the mechanisms did not yield obvious reasons for this variation.

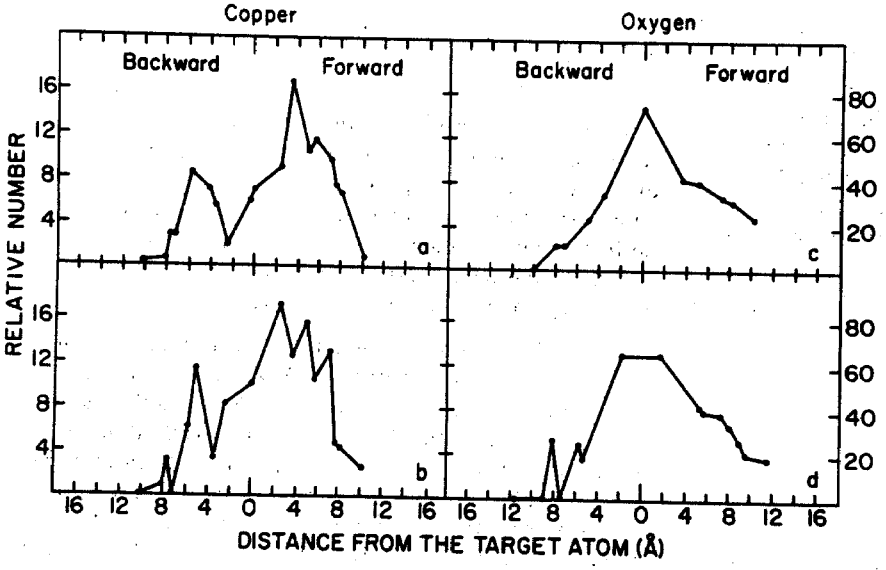

FIG. 9. Relative number of particles ejected versus distance from target atom: Oxygen on Cu(001). (See explanation of Fig. 3.) (a) Cu, $\theta = 45°$, $\phi = 0°$; (b) Cu, $\theta = 45°$, $\phi = 45°$; (c) O, $\theta = 45°$, $\phi = 0°$; (d) O, $\theta = 45°$, $\phi = 45°$.

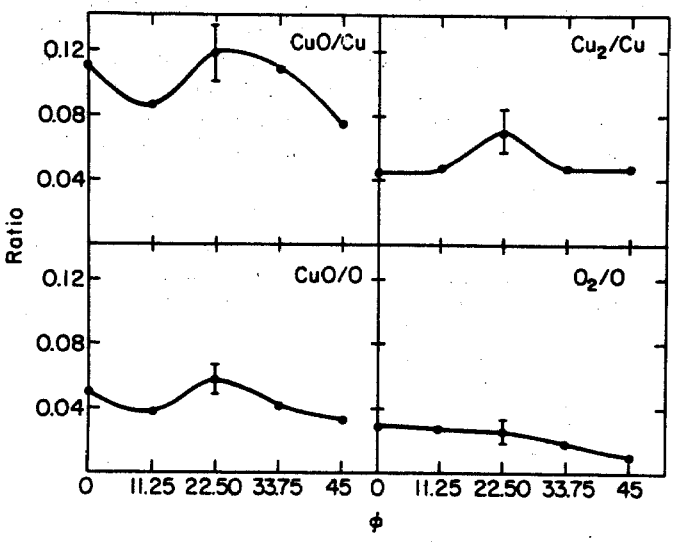

FIG. 10. Dimer to monomer ratios for oxygen on Cu(001) vs ϕ, for $\theta = 45°$.

C. Angular distributions

The angular distributions of the ejected copper and oxygen atoms are shown in Fig. 11. Only the copper atoms with greater than 10 eV of kinetic energy and oxygen atoms with more than 5 eV of kinetic energy are plotted. The copper patterns [Figs. 11(a)–(c)] are very similar to those for the clean metal case [Figs. 8(d)–(f)], except the regions of high intensity are slightly broadened. As in the normal incidence case, the patterns broaden due to the oxygen adsorbate. [15]

The angular distributions of simple adsorbates have been proposed as a means of determining the original site symmetry. [15] In previous work we have shown that the angular distributions of adsorbed oxygens are different depending on whether the oxygen is in an A-top or linearly bonded site, a twofold bridge site, or a fourfold bridge site. [15] The neighboring atoms strongly influence the ejection direction of the adsorbates. For the ejection of oxygen atoms due to oblique angles of incidence of the Ar^+ ion, we find the angular distributions basically unchanged [Figs. 11(d)–(f)]. The patterns are ~45° out of phase. That is, a region of high yield on the O pattern is a region of low yield on the Cu pattern. This indicates that the relationship between the substrate and adsorbate structures continues to be the dominant influence on these angular distributions.

V. SUMMARY AND CONCLUSIONS

In this study we have examined the effect of the angle of incidence of the incoming primary ion on the particle ejection process. By varying the angle of incidence of the primary ion both macroscopic quantities such as yields and microscopic quantities such as mechanisms are altered. In particular we have examined the effect of changing the initial direction of 600 eV Ar^+ ions on clean Cu(001) and Cu(001) with a $c(2\times2)$ coverage of an atomic adsorbate with the mass of oxygen.

The calculated yield of particles ejected from clean Cu(001) as a function of polar angle in the ⟨100⟩ azimuthal directions agree qualitatively with experiment. Of microscopic interest is that at a polar angle of 45° in the ⟨100⟩ directions we find that a shearing

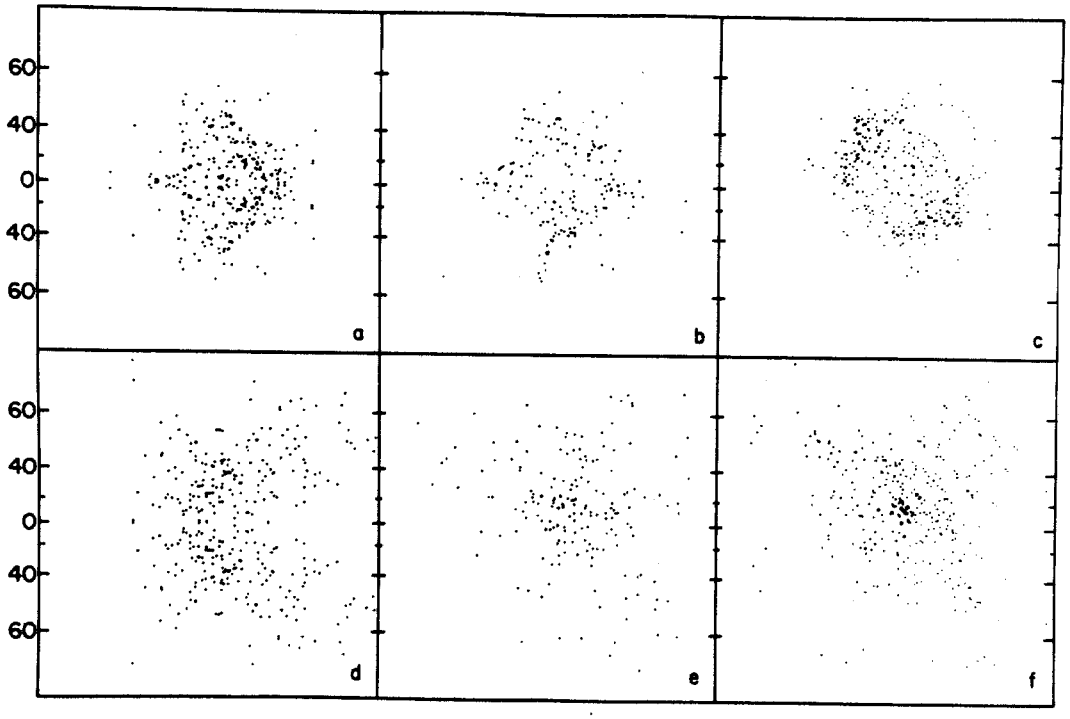

FIG. 11. Angular distributions of ejected copper and oxygen atoms. Only the copper atoms with greater than 10 eV of kinetic energy and oxygen atoms with greater than 5 eV of kinetic energy are shown. (See explanation with Fig. 8.) (a) Cu, $\theta = 45°$, $\phi = 0°$; (b) Cu, $\theta = 45°$, $\phi = 22.5°$; (c) Cu, $\theta = 45°$, $\phi = 45°$; (d) O, $\theta = 45°$, $\phi = 0°$; (e) O, $\theta = 45°$, $\phi = 22.5°$; (f) O, $\theta = 45°$, $\phi = 45°$.

mechanism can occur. That is, one of the struck Cu atoms moves between the first and second layers ejecting the atoms in the first layer. The dependence of the yields on the azimuthal direction for a fixed polar angle of 45° is also given for both clean Cu(001) and the $c(2\times2)$ coverage of oxygen on Cu(001).

For the clean Cu(001) the dimer to monomer ratio is examined as a function of both polar and azimuthal angles. This ratio changes by as much as a factor of 2 from one angle to another. These large changes can be ascribed to dimer formation mechanisms that are specific to given directions of the primary ion. For example, at a polar angle of 45° in the ⟨100⟩ directions, the shearing mechanism accounts for the formation of several dimers that originated from next nearest neighbors on the surface. In the ⟨110⟩ directions, however, there is no shearing and the majority of the dimers originate from atoms that were nearest neighbors on the surface. By energy selecting the ejected dimers one can preferentially enhance the relative number of nearest or next nearest neighbor dimers thus gaining information about the surface structure.

The angular distributions of particles ejected from ion bombarded surfaces has previously been shown to strongly reflect the original site symmetry. We find for oblique angles of incidence of the primary ion, that although the intensity of particles ejected shifts in the direction of the incoming ion, the azimuthal distribution is controlled by the site symmetry.

ACKNOWLEDGMENTS

This research was partially supported by the National Science Foundation (Grant No. 78-08728), the U. S. Air Force Office of Scientific Research (Grant No. AF 76-2974), and the National Resource for Computation in Chemistry under a grant from the National Science Foundation and the Basic Energy Sciences Division of the United States Department of Energy (No. W-7405-ENG-48). Portions of the computations done at Purdue University Computing Center were supported by the President's Reserve Fund. Helpful discussions with N. Winograd and D. E. Harrison, Jr. are also acknowledged.

[1]G. Carter and J. S. Colligon, *Ion Bombardment of Solids* (Elsevier, New York, 1968), and references cited therein.
[2]D. E. Harrison, Jr., W. L. Moore, Jr., and H. T. Holcombe, Radiat. Eff. 17, 167 (1973).
[3]D. E. Harrison, Jr., P. W. Kelly, B. J. Garrison, and N. Winograd, Surface Sci. 76, 311 (1978).
[4]N. Winograd, D. E. Harrison, Jr., and B. J. Garrison, Surface Sci. 78, 467 (1978).
[5]B. J. Garrison, N. Winograd, and D. E. Harrison, Jr., Phys. Rev. B 18, 6000 (1978).
[6]N. Winograd, B. J. Garrison, and D. E. Harrison, Jr., Phys. Rev. B (submitted).
[7]N. Winograd, B. J. Garrison, T. Fleisch, W. N. Delgass, and D. E. Harrison, Jr., J. Vac. Sci. Tech. 16, 629 (1979).
[8]M. Barber and J. C. Vickerman, presented at the First International Conference on Secondary Ion Mass Spectrometry, Münster, West Germany, September, 1977.
[9]N. Winograd and B. Garrison (unpublished results).
[10]D. E. Harrison, Jr., W. L. Gay, and H. M. Effron, J. Math. Phys. 10, 1179 (1969).
[11]The modification follows the procedure of W. H. Miller and T. F. George, J. Chem. Phys. 56, 5668 (1972).
[12]D. Onderdelinden, Thesis, Leiden, 1968, p. 33. Data actually obtained from Harrison, *et al.*, Ref. 2.
[13]B. J. Garrison, N. Winograd, and D. E. Harrison, Jr., J. Chem. Phys. 69, 1440 (1978).
[14]B. J. Garrison, N. Winograd, and D. E. Harrison, Jr., Surface Sci. 87, 101 (1979).
[15]N. Winograd, B. J. Garrison, and D. E. Harrison, Jr., Phys. Rev. Lett. 41, 1120 (1978).
[16]S. P. Holland, B. J. Garrison, N. Winograd, Phys. Rev. Lett. 43, 220 (1979).